JACS
JOURNAL OF THE AMERICAN CHEMICAL SOCIETY
pubs.acs.org/JACS
Article

Potentiometric Measurement to Probe Solvation Energy and Its Correlation to Lithium Battery Cyclability

Sang Cheol Kim, Xian Kong, Rafael A. Vilá, William Huang, Yuelang Chen, David T. Boyle, Zhiao Yu, Hansen Wang, Zhenan Bao, Jian Qin, and Yi Cui*

Cite This: J. Am. Chem. Soc. 2021, 143, 10301−10308
Read Online
ACCESS | Metrics & More | Article Recommendations | Supporting Information

ABSTRACT: The electrolyte plays a critical role in lithium-ion batteries, as it impacts almost every facet of a battery's performance. However, our understanding of the electrolyte, especially solvation of Li^+, lags behind its significance. In this work, we introduce a potentiometric technique to probe the relative solvation energy of Li^+ in battery electrolytes. By measuring open circuit potential in a cell with symmetric electrodes and asymmetric electrolytes, we quantitatively characterize the effects of concentration, anions, and solvents on solvation energy across varied electrolytes. Using the technique, we establish a correlation between cell potential (E_{cell}) and cyclability of high-performance electrolytes for lithium metal anodes, where we find that solvents with more negative cell potentials and positive solvation energies—those weakly binding to Li^+—lead to improved cycling stability. Cryogenic electron microscopy reveals that weaker solvation leads to an anion-derived solid-electrolyte interphase that stabilizes cycling. Using the potentiometric measurement for characterizing electrolytes, we establish a correlation that can guide the engineering of effective electrolytes for the lithium metal anode.

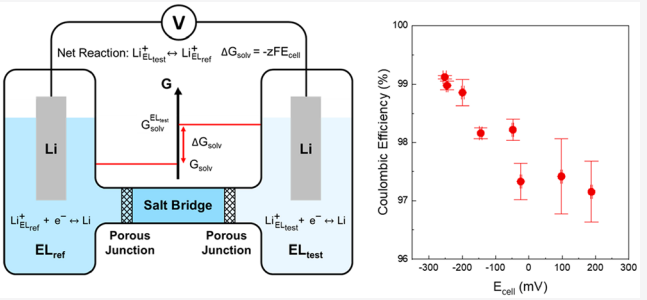

INTRODUCTION

In today's lithium-ion batteries, the electrolyte's role extends beyond simply solvating and transporting Li^+. The electrolyte impacts many aspects of a battery's performance including fast charging capabilities, cycle and calendar life, low-temperature performance, and safety.[1,2] This significance makes the precise formulation of solvents, salts, and additives a highly valuable proprietary information among battery manufacturers.[3] However, our understanding of the electrolyte falls far behind its significance. In particular, the solvation of Li^+, which has profound imprints on many aspects of battery operation such as charge-transfer kinetics, electrolyte bulk transport properties, and solid-electrolyte interphase (SEI),[1,2,4,5] remains elusive. Various spectroscopic techniques have been deployed to study the solvation of Li^+.[6−9] Although these methods provide rich spectroscopic information on local binding structures, it still remains a challenge to quantitatively compare across a large number of electrolytes. To pick out a single metric that is relevant across a wide spectrum of electrolytes is a complex problem. In addition, the analysis often involves complicated deconvolution and interpretation of the spectra, which is not standardized across methodologies, and the presence of the same functional group in different solvents in a mixed-solvent system also adds to the challenge.[10] A single, quantifiable metric is desirable to facilitate the direct comparison of the solvation properties across varied electrolyte formulations.

In this article, we introduce a potentiometric method to probe the Li^+ solvation energy in lithium battery electrolytes. In a galvanic cell with symmetric electrodes but asymmetric electrolytes, we measure the open circuit potential that is correlated to the Li^+ solvation energy relative to a reference electrolyte. The measurement is fast and circumvents the need for costly instruments and complex data analyses, offering an efficient and accessible characterization method. The technique is quantitative and applicable across a wide spectrum of formulations, which enables cell potential (E_{cell}) of the asymmetric electrolyte cell to serve as a metric for characterizing electrolytes. We demonstrate this potential through a correlation between E_{cell} and Coulombic efficiency—a measure of discharge capacity over charge capacity that is representative of the cycling performance of batteries—of high-performance electrolytes for lithium metal anodes. We find that those with a more negative cell potential and weaker Li^+ solvation is desired for superior cycling performance.

Determination of the solvation free energy of ions—the free energy change upon solvating an ion in solution—is a classic

Received: April 13, 2021
Published: June 29, 2021

https://doi.org/10.1021/jacs.1c03868
J. Am. Chem. Soc. 2021, 143, 10301−10308

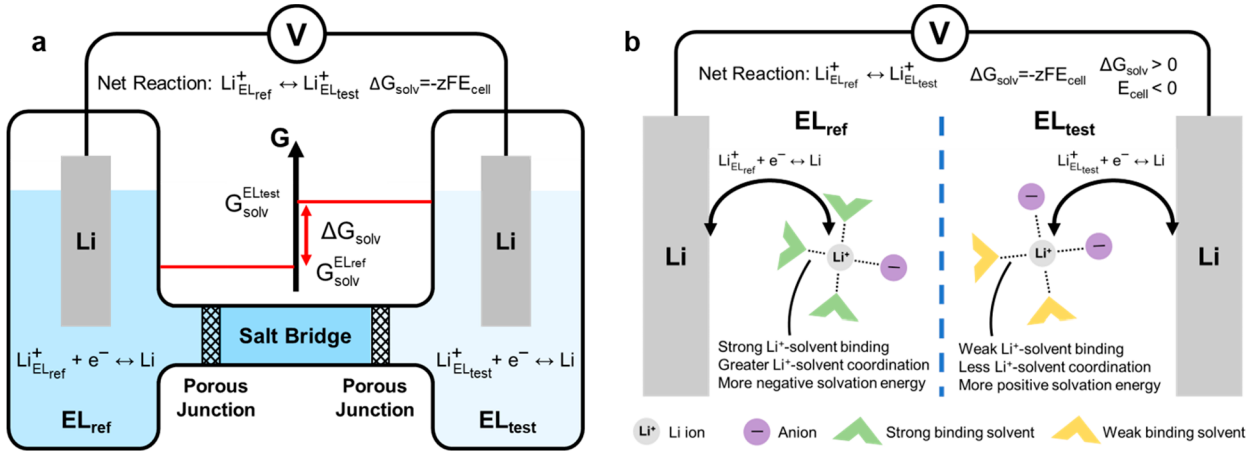

Figure 1. (a) Experimental setup has two half-cells, each with lithium metal as electrode material and two different electrolytes, EL_{ref} and EL_{test}. The difference in the solvation energies of Li^+ (ΔG_{solv}) manifests as the cell voltage (E_{cell}). (b) Model experiment illustrating the relationship between solvation energy and structure. The solvent that binds stronger to Li^+—one with more negative solvation energy—will have higher coordination with Li^+.

problem. It has attracted attention from a fundamental perspective as well as for applications ranging from physiology to textiles.[11] In fact, a methodology to measure relative solvation energy, or the free energy of transfer, was developed decades ago,[11,12] but it has received little attention from the battery community. Potentiometry, an electrochemical method that measures electrical potential at open circuit to probe chemical systems, is at the core of this technique; the technique is used widely in systems such as the galvanic cell,[13] pH meter,[14] and concentration cells.[15,16] Here we present an experimental setup to probe the relative solvation energies of Li^+ in battery electrolytes.

RESULTS

Principles of the Potentiometric Measurement. In an electrochemical system for a reversible process, free energy change of a chemical reaction (ΔG) can be translated into an electrical potential (E) and vice versa, through the relationship $\Delta G = -zFE$,[13] where z is the number of electrons transferred and F is the Faraday constant. In a conventional lithium-ion battery, the electromotive force (EMF) originates from the differences in free energy between two distinct electrodes. On the contrary, in our measurement, EMF is created by free energy differences of Li^+ solvated in two different electrolytes, with the same electrode on both sides. Our cell is composed of two half-cells, each containing a Li metal electrode (Figure 1a). The half cells are filled with two different electrolytes, labeled EL_{ref} (reference electrolyte) and EL_{test} (test electrolyte), connected by a salt bridge. The following half reactions occur at the electrodes, resulting in the following net reaction:

$$Li^+_{EL_{ref}} + e^- \leftrightarrow Li \quad (1)$$

$$Li^+_{EL_{test}} + e^- \leftrightarrow Li \quad (2)$$

$$\text{net reaction: } Li^+_{EL_{ref}} \leftrightarrow Li^+_{EL_{test}} \quad (3)$$

The potential E of the net reaction depends on the free energy differences of Li^+ in the two different electrolytes, because that of metallic Li phase is canceled out. This argument is equivalent to the reason why the electrolyte phase does not affect the potential of a conventional battery, where the effect of electrolyte on the potential is canceled out in the net reaction. Therefore, the cell potential (E_{cell}) at open circuit is a manifestation of the differences in Li^+ solvation free energies in the two electrolytes. Drawing comparisons with our recent work on measuring temperature coefficients in thermocells,[17] EMF in that work was created by establishing a free energy gradient through temperature difference. In the present measurement, free energy gradient arises from entropic and enthalpic differences in the electrolyte at the same temperature. It is worth noting that in this discussion, the term "solvation free energy" refers to the change in free energy in transferring Li^+ in isolated state in vacuum into the electrolyte solution.[11] It essentially captures the chemical potential of Li^+, which is not limited to dilute solutions and captures all factors that contribute to the dissolution of Li^+, including Born solvation, ideal mixing and excess chemical potential, the latter two depending on concentration. The derivation of the cell potential is detailed in Discussion S1.

To accurately and reliably capture the effects of solvation energy on E_{cell}, there are two key experimental design considerations. First, mixing of electrolytes should not affect our results. A porous junction is used to minimize mixing, and we see no appreciable voltage drift within the short measurement time frame of less than 3 minutes (Discussion S2, Figure S1). Second, the liquid junction potential (LJP) must be minimized. LJP is the electrostatic potential difference at the interface between two solutions that arise from the discrepancies in transference numbers of the ions.[13] The problem of LJP and its treatment are well established:[13] it can be minimized through the implementation of a salt bridge, using a high concentration electrolyte that has equal transference numbers of cations and anions.[18,19] The salt bridge electrolyte—because of its high activity—dominates the LJP and creates equal and opposite potentials at the two junctions, resulting in net zero liquid junction potential (Discussion S3).[13]

Formation of a solid-electrolyte interphase (SEI) layer on the electrode is another factor that needs to be considered. SEI forms spontaneously on Li metal electrodes in a liquid electrolyte environment, and the effects of different SEIs

https://doi.org/10.1021/jacs.1c03868
J. Am. Chem. Soc. 2021, 143, 10301−10308

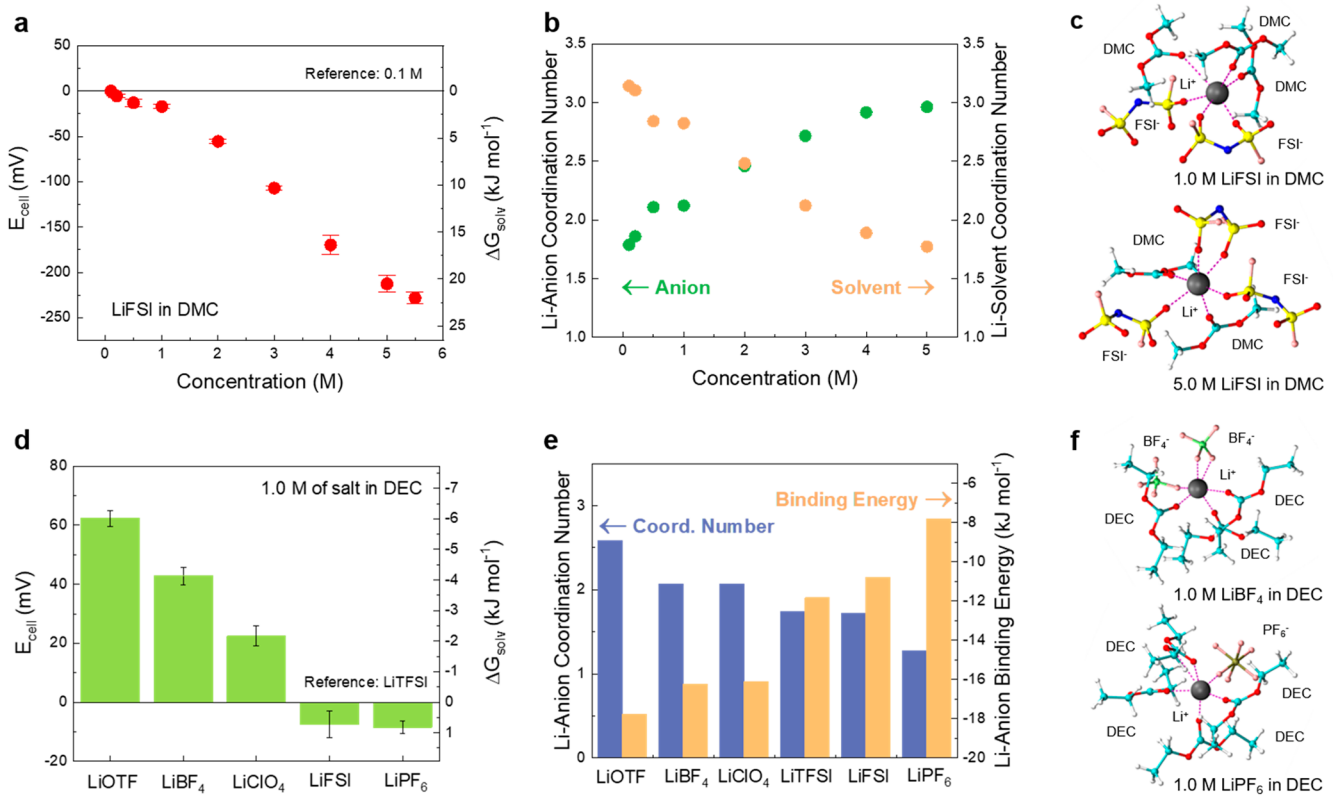

Figure 2. (a) Measured cell potentials at different concentrations of LiFSI in DMC. Cell potential decreases with concentration, signifying more positive solvation energy and weaker solvation at high concentrations. (b) MD simulation results on the coordination number showing that coordination with solvent is weakened and coordination with anion is more pronounced as concentration increases. (c) Simulated solvation structures at concentrations of 1.0 and 5.0 M LiFSI in DMC. More anions and fewer solvents are coordinated with Li^+ at 5.0 M than 1.0 M. (d) Measured cell potentials of various salts of 1.0 M concentration in DEC. Compared with TFSI, OTF^-, BF_4^-, and ClO_4^- show stronger binding with Li^+, whereas FSI^- and PF_6^- show weaker binding. (e) MD simulation results of Li-anion binding energy and coordination numbers. Binding energy shows the same trend as the solvation energy measurements, and the Li-anion coordination number shows a decreasing trend with weaker binding. (f) Simulated solvation structures of 1.0 M $LiBF_4$ in DEC and 1.0 M $LiPF_6$ in DEC. PF_6^- has weaker binding with Li^+ than BF_4^-, and consequently less ion-pairing.

formed from different electrolytes on the potential measurement must be verified (Discussion S4, Figures S2 and S3). We preformed different SEIs on the Li electrodes by immersing them into different electrolytes for 48 h, and constructed a symmetric cell with a single electrolyte, but the different preformed SEIs. In the case of SEI affecting cell potential, we expect the different SEIs to create asymmetric effects and thus observe an EMF. However, we observe no EMF (Figure S2) and negligible effects of SEI on our measurements. Further explanation of this effect from a fundamental perspective is detailed in Discussion S4.

Solvation energy is intricately interconnected with solvation structure, as the electrolyte components will reconfigure to assume the lowest energy solvation structure. Figure 1b depicts a model experiment that illustrates the relationship between solvation energy and structure. Let us assume that two different solvents are used in the two electrolytes, EL_{ref} and EL_{test}, and the open circuit potential measurement yields a negative electrical potential. More negative electric potential signifies more positive free energy of solvation, and weaker binding of solvent to Li^+. Under the condition that the total coordination number—the combined number of anions and solvents in the solvation structure—stays relatively constant, weaker solvent binding implies a lower Li^+-solvent coordination, as illustrated in Figure 1b. In general, as will be confirmed in later parts of this discussion, an electrolyte that has a more negative E_{cell} infers a more positive solvation energy and a weaker binding between the components of the solvation shell and Li^+, which subsequently affects the solvation structure.

Anion and Concentration Effect on Solvation. We proceeded to apply our methodology to quantify the effect of salt concentration on solvation energy. Salt concentration, especially with the introduction of high concentration electrolytes (HCE), has emerged as an effective tuning parameter for engineering high-performance electrolytes.[4,20] At high concentrations, electrolytes possess strikingly different properties, including superior cycling stability for lithium metal anodes,[20] oxidative stability, and improved safety,[4] effects of which are closely tied with Li^+ solvation. Figure 2a and Table S1 show the measured solvation energy with different salt concentrations, using lithium bis(fluorosulfonyl)imide (LiFSI) salt in dimethyl carbonate (DMC), measured versus a reference electrolyte of 0.1 M LiFSI in DMC. We find that increasing the concentration leads to more negative cell potentials, inferring more positive solvation energies; the value for 5.5 M solution is more negative than the 0.1 M reference solution by about 220 mV. This trend is in accordance with the Nernst equation, which predicts a more negative potential and a more positive free energy at higher concentrations. It is worth reiterating that in this discussion, the term "solvation free

https://doi.org/10.1021/jacs.1c03868
J. Am. Chem. Soc. 2021, 143, 10301−10308

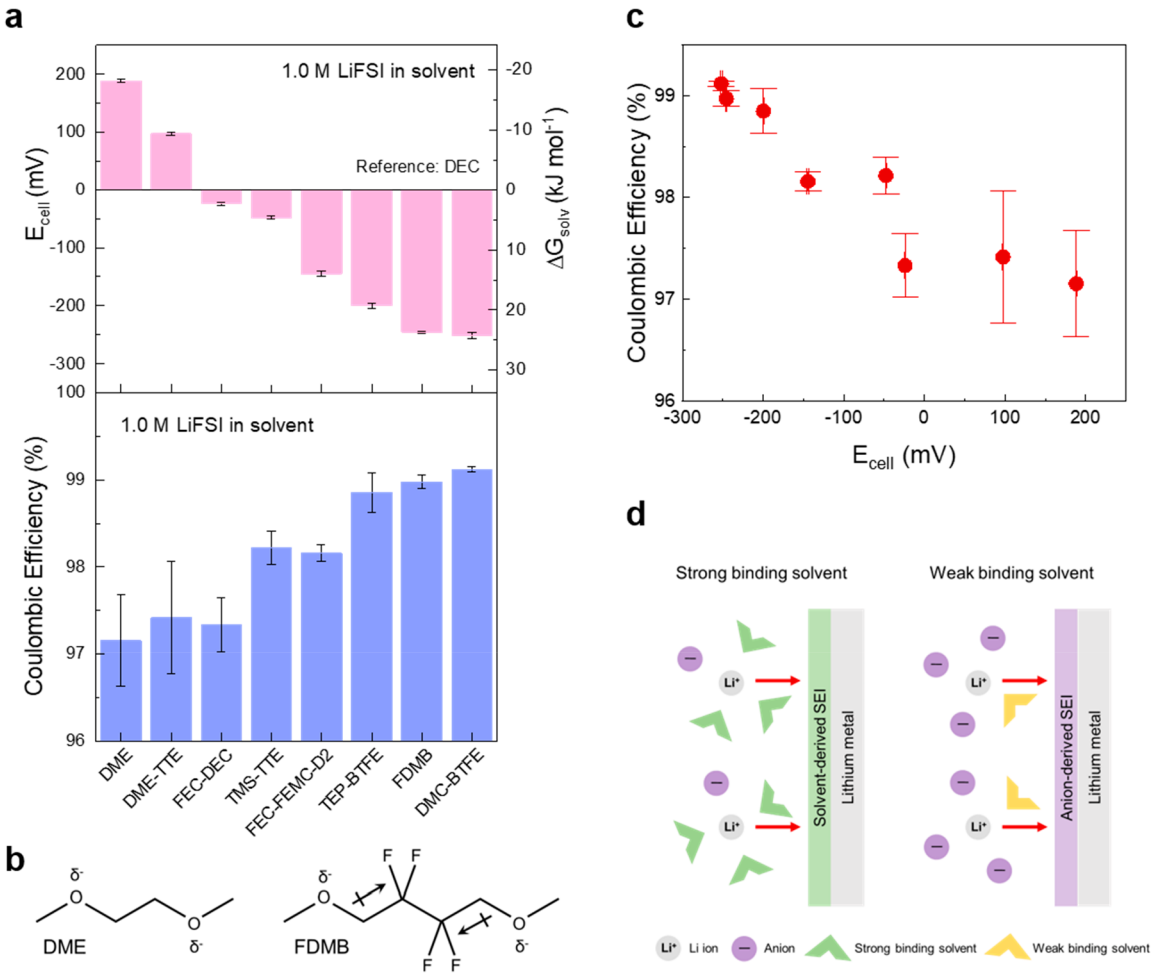

Figure 3. Solvation energy and CE of high-performance electrolytes for lithium metal anode. (a) Solvation energy and Coulombic efficiencies (CE) of eight different high-performance electrolytes. (b) Chemical structures of DME and FDMB solvents. (c) CE vs solvation energy of the electrolytes in Figure 3a. It shows a positive correlation, signifying more positive solvation energy and weaker binding solvent leads to superior CE. (d) Schematic illustrating the relationship between solvent binding and structure, and SEI formed in electrolytes. Weak binding solvents increase Li^+-anion coordination, which consequently leads to anion-derived SEI, which is believed to have superior cycling performance for the lithium metal anode.

energy" is not limited to dilute solutions and includes the effects from concentration.

Molecular dynamics (MD) simulations illustrate the effect of concentration on the solvation structures (Figure 2b and Table S2). We find that at elevated concentrations, solvent species in the solvation shell of Li^+ are replaced with anions. For instance, as illustrated in Figure 2c, an average Li-solvent coordination number is reduced to 2 at 5.0 M from 3 at 1.0 M (Figure S4). Similar trends were found by Wan et al.[9] and Flores et al.[21] It can be inferred that at low concentrations, Li^+-solvent binding is favored over Li^+-anion binding, particularly as FSI^- is a highly dissociated anion that interacts weakly with Li^+, a finding presented in the following discussions. However, at higher concentrations, the ratio between the solvent and salt decreases, and the system does not have sufficient solvent molecules to solvate Li^+. More anions participate in the Li^+ solvation shell, which is less favorable than a more solvent-dominated counterpart, leading to a more positive solvation energy as well as the Li^+ activity coefficients (Figure S5).

The type of anions is another key parameter in electrolyte engineering. Different anions have differing degrees of ion dissociation, which significantly impacts the transport properties.[1] Ion dissociation is expected to be intricately related to Li^+ solvation; anions that have strong binding energies to Li^+ and more negative solvation energies will have increased ion-pairing and lower ion dissociation. Figure 2d and Table S3 show the free energy of solvation for a series of salts dissolved in a common solvent of diethyl carbonate (DEC). Salt concentration is fixed at 1.0 M and all electrolytes were measured against a reference electrolyte of 1.0 M LiTFSI in DEC. The data show that differences in cell potentials for different anions are significant; compared with bistriflimide ($TFSI^-$) anion, triflate (OTF^-), tetrafluoroborate (BF_4^-), and perchlorate (ClO_4^-) have significantly more positive cell potentials and more negative solvation energies, whereas bis(fluorosulfonyl)imide (FSI^-) and hexafluorophosphate (PF_6^-) show slightly more positive solvation energies. It can be inferred that strongly binding anions such as OTF^- and BF_4 will be bound to Li^+ to a larger degree than weakly binding ones like FSI^- and PF_6^-. The results are corroborated by MD simulation: simulated Li-anion binding free energies match with our experimental results (Figure 2e). Simulation results also elucidate the relationship between solvation energy and structure; strongly binding anion species occupy a larger share

https://doi.org/10.1021/jacs.1c03868
J. Am. Chem. Soc. 2021, 143, 10301−10308

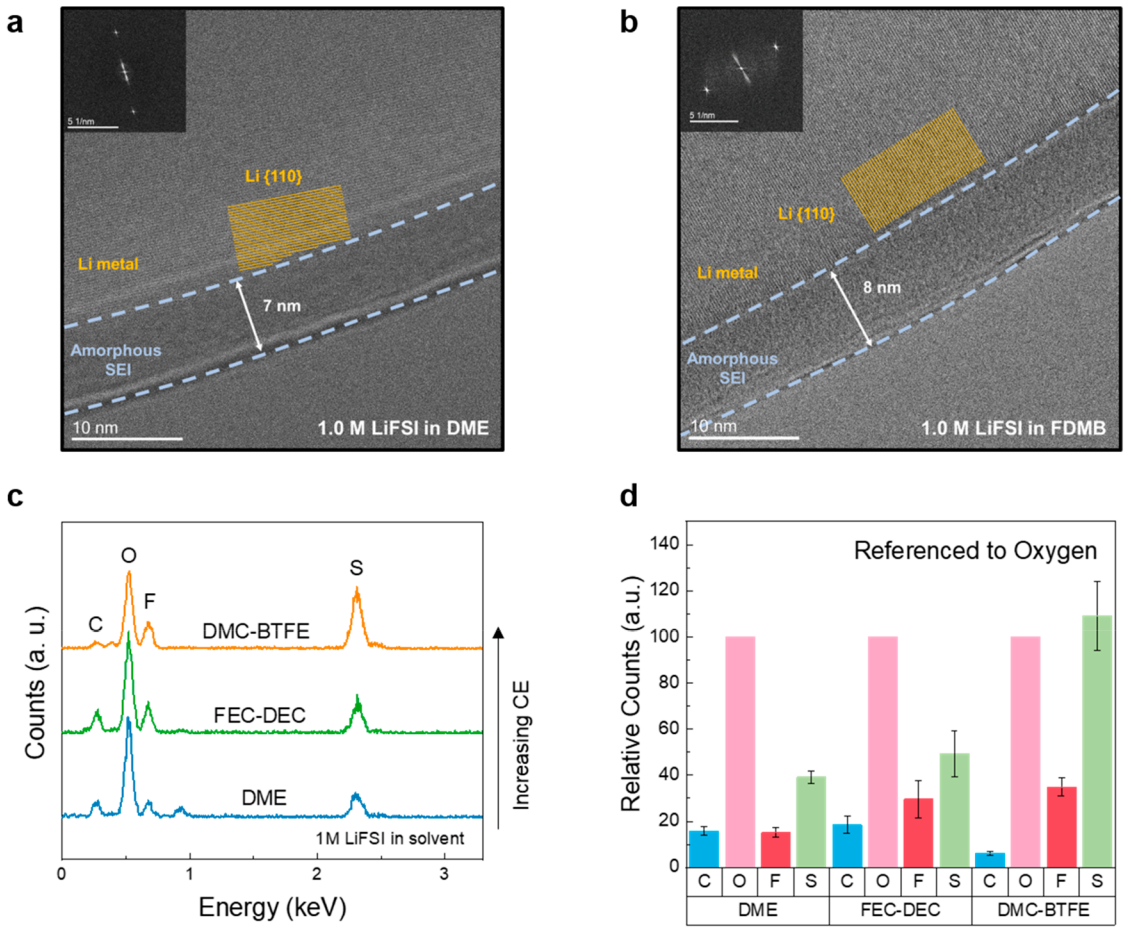

Figure 4. Cryo-EM studies of SEI in various electrolytes. (a, b) HR-TEM images with FFT of SEIs formed in 1.0 M LiFSI in DME and 1.0 M LiFSI in FDMB, respectively. Two show similar SEI structures. (c, d) EDS spectra and quantification of the relative counts of each element for three different electrolytes. Different SEIs show significantly different chemical compositions, and electrolytes with superior CE exhibit higher sulfur content in the SEI.

of the first solvation shell (Figure 2e and Table S4). This trend is illustrated in Figure 2f, where the Li-anion coordination number of BF_4^- is larger than that of FSI^- (Figure S6). These experimental and simulation findings are well-correlated with ion dissociation trends;[5,22,23] anions known to have lower ion dissociation have more negative solvation energies in the same solvent and higher degrees of ion pairing.

Solvent Effect on Solvation and Correlation to Coulombic Efficiency. The development of new solvents has been a major driver for the recent improvements in lithium metal anode cyclability, and solvation of Li^+ is believed to play a crucial role.[4,24−26] We selected representative high-performance electrolyte solvents[24,25,27−31] to systematically study the relationship between solvation energy and Li metal cyclability. Figure 3a and Table S5 show the measured open circuit cell potentials and Coulombic efficiencies (CE) of these representative electrolyte solvents. To isolate the effect of the solvent, LiFSI salt at 1.0 M concentration is used in all electrolytes.

Plotting CE versus E_{cell}, we find a clear negative correlation: solvents with more negative potentials and more positive solvation energies exhibit superior cycling performance (Figure 3c). This trend is consistent with previous reports;[32−34] weakly solvating solvents promote increased participation of FSI^- in the solvation structure (Figure S7). Solvation structure is hypothesized to significantly impact the SEI composition.[32] Increased Li^+-FSI^- coordination may lead to heightened decomposition of the anion at the anode interface, leading to an anion-derived SEI rather than a solvent-derived one (Figure 3d).[32] A similar trend is observed for high-concentration electrolytes (HCE). HCEs, which are known to have excellent cycling stability for Li metal anodes,[20] were shown earlier in this discussion to also exhibit highly positive solvation energies and increased Li^+-anion coordination. Our findings suggest, therefore, that electrolytes with highly positive solvation energies, enabled through weakly solvating solvents or high salt concentrations, can lead to improved cyclability of Li metal anodes. A caveat may be that weaker solvation can lead to a decrease in salt solubility and inferior ionic conductivity. Therefore, it is important to strike a balance between Coulombic efficiency and ion transport. It is also worth noting that in the case of poor electrolytes that form solvent-derived SEI, solvent properties such as reductive stability and the ability to form a passivating SEI may become more dominant factors of the cycling stability.

The large differences in solvation energy among the different electrolytes can be related to the molecular structures—particularly the effect of fluorination—of the solvents. DME and FDMB have comparable molecular structures; both contain two ethereal oxygens, but FDMB is fluorinated with

https://doi.org/10.1021/jacs.1c03868
J. Am. Chem. Soc. 2021, 143, 10301−10308

a slightly longer carbon backbone (Figure 3b). However, the two solvents exhibit a strikingly large difference in cell potentials of more than 400 mV, and such a difference is expected to have a major impact on the battery performance. A large portion of this energy difference is conjectured to arise from the inductive effect of fluorine, where the highly electronegative fluorine atom pulls in the electron cloud and decreases the polarity of oxygen species that interacts with Li^+.[35] Therefore, fluorine decoration on solvent molecules can be a promising strategy to weaken Li^+ solvation and promote superior cycling stability. The comparison of DME and DME-TTE also shows that the use of fluorinated cosolvents, such as 1,1,2,2-tetrafluoroethyl-2,2,3,3-tetrafluoropropyl ether (TTE), is another strategy to weaken Li^+ solvation and lead to heightened cyclability. This is in accord with the concept of local high concentration electrolytes proposed by Zhang, Xu and co-workers.[25,29] Because fluorinated cosolvents do not directly participate in the solvation of Li^+, they effectively increase the concentration of salt in the main solvent, and this leads to weaker solvation as was seen in our prior discussion on high concentration electrolytes (Figure 2a).

Cryo-EM Characterization of SEI. To investigate the possible causes of the relationship between CE and solvation energy, we characterized the SEI using cryogenic electron microscopy (cryo-EM). Cryo-EM is a unique tool for characterizing beam-sensitive battery materials, including Li metal and its SEI, because it enables us to directly visualize and analyze the structural and chemical characteristics of the SEI with nanoscale resolution.[36,37] SEI is highly heterogeneous at the nanoscale, with the presence of compact SEI as well as extended SEI.[38,39] Huang et al. also recently discovered that lithium fluoride (LiF)—an integral constituent of the SEI—exists as local particulates rather than as a conformal film.[40] It is therefore important to analyze and make comparisons between each component of the SEI at the nanoscale.

Here we have characterized the compact SEI—a thin passivating film that conformally forms on the interface—of different electrolytes using cryo-EM. In Figure 4a, b, we compare the SEIs formed in 1.0 M LiFSI in DME, a commonly used electrolyte, and 1.0 M LiFSI in FDMB, representative of a high-performing electrolyte. The HR-TEM images of the two SEIs are surprisingly similar, both having a thin, homogeneous SEI of about 7−8 nm. Furthermore, both SEIs are fully amorphous without any crystalline domains, characteristic of the monolithic SEI structure observed previously.[31,41] This is validated by the fast-Fourier transforms (FFT): Li{110} is the only signal present in the FFT pattern. Structurally, we see no discernible differences between the two interphases.

On the contrary, the chemical information revealed by energy-dispersive X-ray spectroscopy (EDS) shows clear differences, where anion-derived species dominate the SEI formed in high-performing electrolytes. Figure 4c, d show the elemental analyses of three different SEIs revealed by EDS using cryo-EM (Table S6). Among the four elements, we focus on sulfur, because it can serve as a proxy for anion-derived SEI: FSI^- being the sole species containing sulfur, higher sulfur content translates to more anion-derived SEI. The results show marked differences in sulfur content, increasing in the order of increasing CE. These findings provide evidence in support of the mechanism illustrated in Figure 3c; weakly binding solvents lead to higher anion coordination with Li^+, which then leads to a more anion-derived SEI that promotes the cycling performance of lithium metal anodes. The anion-rich solvation structure may also lead to an upward shifting of the reduction potential of anions,[4] which renders them more prone to reduction and contributes to an anion-derived SEI.

CONCLUSION

This report presents a potentiometric method to probe the relative solvation energy in lithium battery electrolytes and demonstrates its applicability to electrolytes of a wide spectrum of salt concentrations, anions, and solvent chemistries. To illustrate its potential as a metric for characterizing the electrolyte, we correlated cell potentials of the asymmetric electrolyte cell with Li metal cyclability, where a clear negative correlation was found. Our findings suggest that further discovery of electrolyte architectures with weak Li^+ solvation, for example, through the use of fluorinated solvents, can lead to advancements in Li metal cyclability. Our methodology can be utilized to efficiently screen electrolyte formulations to expedite the search for novel high-performance electrolytes. In addition, we anticipate solvation energy to be closely tied with other performance metrics such as charge-transfer impedance and for further studies to lead to new insights and design principles for engineering electrolytes in the future.

ASSOCIATED CONTENT

Supporting Information

The Supporting Information is available free of charge at https://pubs.acs.org/doi/10.1021/jacs.1c03868.

Experimental methods, supplementary discussion of the experimental principles, potentiometric data on measurement setup, supporting data on simulations, and tables summarizing measurement results (PDF)

AUTHOR INFORMATION

Corresponding Author

Yi Cui − *Department of Materials Science and Engineering, Stanford University, Stanford, California 94305, United States; Stanford Institute for Materials and Energy Sciences, SLAC National Accelerator Laboratory, Menlo Park, California 94025, United States;* orcid.org/0000-0002-6103-6352; Email: yicui@stanford.edu

Authors

Sang Cheol Kim − *Department of Materials Science and Engineering, Stanford University, Stanford, California 94305, United States;* orcid.org/0000-0002-1749-8277

Xian Kong − *Department of Chemical Engineering, Stanford University, Stanford, California 94305, United States;* orcid.org/0000-0001-5602-6347

Rafael A. Vilá − *Department of Materials Science and Engineering, Stanford University, Stanford, California 94305, United States*

William Huang − *Department of Materials Science and Engineering, Stanford University, Stanford, California 94305, United States;* orcid.org/0000-0001-8717-5337

Yuelang Chen − *Department of Chemistry, Stanford University, Stanford, California 94305, United States*

David T. Boyle − *Department of Chemistry, Stanford University, Stanford, California 94305, United States;* orcid.org/0000-0002-0452-275X

Zhiao Yu − *Department of Chemistry, Stanford University, Stanford, California 94305, United States;* orcid.org/0000-0001-8746-1640

Hansen Wang − *Department of Materials Science and Engineering, Stanford University, Stanford, California 94305, United States;* orcid.org/0000-0002-6738-1659
Zhenan Bao − *Department of Chemical Engineering, Stanford University, Stanford, California 94305, United States;* orcid.org/0000-0002-0972-1715
Jian Qin − *Department of Chemical Engineering, Stanford University, Stanford, California 94305, United States;* orcid.org/0000-0001-6271-068X

Complete contact information is available at: https://pubs.acs.org/10.1021/jacs.1c03868

Notes

The authors declare no competing financial interest.

■ ACKNOWLEDGMENTS

R.A.V. acknowledges support from the National Academy of Sciences Ford Foundation Fellowship and the National Science Foundation Graduate Research Fellowship Program (NSF GRFP, grant DGE 1656518). D.T.B. acknowledges the National Science Foundation Graduate Research Fellowship Program (NSF GRFP) for funding. The cryo-EM part is supported by the Department of Energy, Office of Basic Energy Sciences, Division of Materials Science and Engineering, under contract DE-AC02-76SF00515. The battery and electrolyte measurement part was supported by the Assistant Secretary for Energy Efficiency and Renewable Energy, Office of Vehicle Technologies, of the U.S. Department of Energy under the Battery Materials Research (BMR) Program and the Battery500 Consortium program. Part of this work was performed at the Stanford Nano Shared Facilities (SNSF). The HR-TEM images were taken with a K3 IS camera and support is courtesy of Gatan. The authors acknowledge J. Baek for fruitful discussions and manuscript editing.

■ REFERENCES

(1) Xu, K. Nonaqueous liquid electrolytes for lithium-based rechargeable batteries. *Chem. Rev.* **2004**, *104*, 4303−4417.
(2) Xu, K. Electrolytes and interphases in Li-ion batteries and beyond. *Chem. Rev.* **2014**, *114*, 11503−11618.
(3) An, S. J.; et al. The state of understanding of the lithium-ion-battery graphite solid electrolyte interphase (SEI) and its relationship to formation cycling. *Carbon* **2016**, *105*, 52−76.
(4) Yamada, Y.; Wang, J.; Ko, S.; Watanabe, E.; Yamada, A. Advances and issues in developing salt-concentrated battery electrolytes. *Nat. Energy* **2019**, *4*, 269−280.
(5) Boyle, D. T.; et al. Transient Voltammetry with Ultramicroelectrodes Reveals the Electron Transfer Kinetics of Lithium Metal Anodes. *ACS Energy Lett.* **2020**, *5*, 701−709.
(6) Cresce, A. V.; et al. Solvation behavior of carbonate-based electrolytes in sodium ion batteries. *Phys. Chem. Chem. Phys.* **2017**, *19*, 574−586.
(7) Seo, D. M.; et al. Role of mixed solvation and ion pairing in the solution structure of lithium ion battery electrolytes. *J. Phys. Chem. C* **2015**, *119*, 14038−14046.
(8) Ming, J.; et al. New Insight on the Role of Electrolyte Additives in Rechargeable Lithium Ion Batteries. *ACS Energy Lett.* **2019**, *4*, 2613−2622.
(9) Wan, C.; et al. Natural abundance 17O, 6Li NMR and molecular modeling studies of the solvation structures of lithium bis(fluorosulfonyl)imide/1,2-dimethoxyethane liquid electrolytes. *J. Power Sources* **2016**, *307*, 231−243.
(10) Su, C. C.; et al. Solvating power series of electrolyte solvents for lithium batteries. *Energy Environ. Sci.* **2019**, *12*, 1249−1254.
(11) Marcus, Y. *Ions in Solution and their Solvation. Ions in Solution and their Solvation* **2015**, DOI: 10.1002/9781118892336.
(12) Kundu, K. K.; Parker, A. J. Solvation of ions. XXVII. Comparison of methods to calculate single ion free energies of transfer in mixed solvents. *J. Solution Chem.* **1981**, *10*, 847−861.
(13) Bard, A. J.; Faulkner, L. R. *Electrochemical Methods: Fundamentals and Applications*, 2nd ed; Wiley, 2000.
(14) Spitzer, P.; et al. *Reference Electrodes for Aqueous Solutions. Handbook of Reference Electrodes* **2013**, 77.
(15) Georén, P.; Lindbergh, G. Characterisation and modelling of the transport properties in lithium battery gel electrolytes: Part I. The binary electrolyte PC/LiClO4. *Electrochim. Acta* **2004**, *49*, 3497−3505.
(16) Stewart, S.; Newman, J. Measuring the Salt Activity Coefficient in Lithium-Battery. *J. Electochem. Soc.* **2008**, *155*, 458−463.
(17) Wang, H.; et al. Correlating Li-Ion Solvation Structures and Electrode Potential Temperature Coefficients. *J. Am. Chem. Soc.* **2021**, *143*, 2264.
(18) Suo, L.; Hu, Y. S.; Li, H.; Armand, M.; Chen, L. A new class of Solvent-in-Salt electrolyte for high-energy rechargeable metallic lithium batteries. *Nat. Commun.* **2013**, *4*, 1−9.
(19) Agostini, M.; Scrosati, B.; Hassoun, J. An Advanced Lithium-Ion Sulfur Battery for High Energy Storage. *Adv. Energy Mater.* **2015**, *5*, 1500481.
(20) Qian, J.; Henderson, W. A.; Xu, W.; Bhattacharya, P.; Engelhard, M.; Borodin, O.; Zhang, J.-G. High rate and stable cycling of lithium metal anode. *Nat. Commun.* **2015**, *6*, 6362.
(21) Flores, E.; Åvall, G.; Jeschke, S.; Johansson, P. Solvation structure in dilute to highly concentrated electrolytes for lithium-ion and sodium-ion batteries. *Electrochim. Acta* **2017**, *233*, 134−141.
(22) Seo, D. M.; Borodin, O.; Han, S. D.; Boyle, P. D.; Henderson, W. A. Electrolyte solvation and ionic association II. Acetonitrile-lithium salt mixtures: Highly dissociated salts. *J. Electrochem. Soc.* **2012**, *159*, A1489.
(23) Ue, M.; Mori, S. Mobility and Ionic Association of Lithium Salts in a Propylene Carbonate-Ethyl Methyl Carbonate Mixed Solvent. *J. Electrochem. Soc.* **1995**, *142*, 2577−2581.
(24) Fan, X.; et al. All-temperature batteries enabled by fluorinated electrolytes with non-polar solvents. *Nat. Energy* **2019**, *4*, 882−890.
(25) Ren, X.; et al. Enabling High-Voltage Lithium-Metal Batteries under Practical Conditions. *Joule* **2019**, *3*, 1662−1676.
(26) Amanchukwu, C. V.; Kong, X.; Qin, J.; Cui, Y.; Bao, Z. Nonpolar Alkanes Modify Lithium-Ion Solvation for Improved Lithium Deposition and Stripping. *Adv. Energy Mater.* **2019**, *9*, 1902116.
(27) Chen, S.; et al. High-Efficiency Lithium Metal Batteries with Fire-Retardant Electrolytes. *Joule* **2018**, *2*, 1548−1558.
(28) Ren, X.; et al. Localized High-Concentration Sulfone Electrolytes for High-Efficiency Lithium-Metal Batteries. *Chem.* **2018**, *4*, 1877−1892.
(29) Chen, Y.; Zhang, Y.; Wang, Z.; Zhan, T.; Wang, Y.-C.; Zou, H.; Ren, H.; Zhang, G.; Zou, C.; Wang, Z. L.; et al. High-Voltage Lithium-Metal Batteries Enabled by Localized High-Concentration Electrolytes. *Adv. Mater.* **2018**, *30*, 1−7.
(30) Weber, R.; et al. Long cycle life and dendrite-free lithium morphology in anode-free lithium pouch cells enabled by a dual-salt liquid electrolyte. *Nat. Energy* **2019**, *4*, 683−689.
(31) Yu, Z.; Wang, H.; Kong, X.; Huang, W.; Tsao, Y.; Mackanic, D. G.; Wang, K.; Wang, X.; Huang, W.; Choudhury, S. Molecular design for electrolyte solvents enabling energy-dense and long-cycling lithium metal batteries. *Nat. Energy* **2020**, *5*, 526.
(32) Yao, Y. X.; et al. Regulating Interfacial Chemistry in Lithium-Ion Batteries by a Weakly Solvating Electrolyte**. *Angew. Chem., Int. Ed.* **2021**, *60*, 4090−4097.
(33) Holoubek, J.; Liu, H.; Wu, Z.; Yin, Y.; Xing, X.; Cai, G.; Yu, S.; Zhou, H.; Pascal, T. A.; Chen, Z.; Liu, P. Tailoring electrolyte solvation for Li metal batteries cycled at ultra-low temperature. *Nat. Energy* **2021**, *6*, 303.

(34) Liu, H.; et al. Ultrahigh coulombic efficiency electrolyte enables Li||SPAN batteries with superior cycling performance. *Mater. Today* **2021**, *42*, 17−28.
(35) Henne, A. L.; Smook, M. A. Fluorinated Ethers. *J. Am. Chem. Soc.* **1950**, *72*, 4378−4380.
(36) Li, Y.; et al. Atomic structure of sensitive battery materials and interfaces revealed by cryo−electron microscopy. *Science (Washington, DC, U. S.)* **2017**, *358*, 506−510.
(37) Wang, X.; et al. New Insights on the Structure of Electrochemically Deposited Lithium Metal and Its Solid Electrolyte Interphases via Cryogenic TEM. *Nano Lett.* **2017**, *17*, 7606−7612.
(38) Huang, W.; et al. Evolution of the Solid-Electrolyte Interphase on Carbonaceous Anodes Visualized by Atomic-Resolution Cryogenic Electron Microscopy. *Nano Lett.* **2019**, *19*, 5140−5148.
(39) Zheng, J.; et al. 3D visualization of inhomogeneous multi-layered structure and Young's modulus of the solid electrolyte interphase (SEI) on silicon anodes for lithium ion batteries. *Phys. Chem. Chem. Phys.* **2014**, *16*, 13229−13238.
(40) Huang, W.; Wang, H.; Boyle, D. T.; Li, Y.; Cui, Y. Resolving Nanoscopic and Mesoscopic Heterogeneity of Fluorinated Species in Battery Solid-Electrolyte Interphases by Cryogenic Electron Microscopy. *ACS Energy Lett.* **2020**, *5*, 1128−1135.
(41) Cao, X.; et al. Monolithic solid−electrolyte interphases formed in fluorinated orthoformate-based electrolytes minimize Li depletion and pulverization. *Nat. Energy* **2019**, *4*, 796−805.

https://doi.org/10.1021/jacs.1c03868
J. Am. Chem. Soc. 2021, 143, 10301−10308